Research Square

Preprints are preliminary reports that have not undergone peer review.
They should not be considered conclusive, used to inform clinical practice,
or referenced by the media as validated information.

A Study on the Adsorption Performance of Potassium Bicarbonate-Modified Biochar towards Benzo[a]pyrene in Aquatic Environments

Qian Liu
Huazhong Agricultural University
Yun Yang
Huazhong Agricultural University
Yang Yin
Huazhong Agricultural University
QingLing Fu
Huazhong Agricultural University
Jun Zhu
Huazhong Agricultural University
YongHong Liu
Huazhong Agricultural University
HongQing Hu
hqhu@mail.hzau.edu.cn

Huazhong Agricultural University

Research Article

Keywords: benzo[a]pyrene, porous biochar, polycyclic aromatic hydrocarbon contamination, adsorption, potassium bicarbonate modification

Posted Date: November 12th, 2026

DOI: https://doi.org/10.21203/rs.3.rs-11107605/v1

License: This work is licensed under a Creative Commons Attribution 4.0 International License.
Read Full License

Additional Declarations: No competing interests reported.

A Study on the Adsorption Performance of Potassium Bicarbonate-Modified Biochar towards Benzo[a]pyrene in Aquatic Environments

Qian Liu, Yun Yang, Yang Yin, QingLing Fu, Jun Zhu, YongHong Liu & HongQing Hu(✉)

Abstract: Benzo[a]pyrene (BaP) is a highly carcinogenic and highly mobile polycyclic aromatic hydrocarbon, and there is an urgent need to develop remediation technologies for water bodies contaminated with it. In this study, porous biochar (PBC) was prepared from rice straw using co-pyrolysis with $KHCO_3$ as an activation agent, and its adsorption characteristics and mechanism of action towards BaP in water were investigated. High-temperature etching with $KHCO_3$ creates a rich microporous structure and enhances the aromaticity of the carbon framework; PBC800, prepared at 800℃, exhibits a saturated adsorption capacity of up to 55.41 mg/g; compared with the adsorption capacity of 25.47 mg/g for the original biochar, this represents an increase of 217.55%. Adsorption followed quasi-second-order kinetics and the Langmuir model. The adsorption process is predominantly characterised by spontaneous endothermic physical adsorption, accompanied by weak π-π and electron donor-acceptor interactions, with microporous filling and π-π interactions being the primary mechanisms. Response surface analysis indicated that the factors influencing performance, in order of significance, were: biochar dosage> temperature> initial BaP concentration. Under optimal conditions, the theoretical removal rate was

Q. Liu · Y. Yang · Y. Yin · Q. Fu · J. Zhu · Y. Liu · H. Hu(✉)

Hubei Key Laboratory of Soil Environment and Pollution Remediation,College of Resources and Environment, Huazhong Agricultural University, Wuhan 430070, China

e-mail: hqhu@mail.hzau.edu.cn

Q. Liu

E-mail:lqlqlq6495@163.com

94.08%. The coexistence of carbonates was found to inhibit BaP adsorption; In practical applications involving water bodies, attention must be paid to the concentration of carbonate ions.. This potassium bicarbonate modified biochar provides a theoretical reference for the remediation of BaP pollution in water bodies.

Keywords: benzo[a]pyrene; porous biochar; polycyclic aromatic hydrocarbon contamination; adsorption; potassium bicarbonate modification

1 Introduction

Polycyclic aromatic hydrocarbons(PAHs), as a typical group of hydrophobic organic pollutants (HOPs) (Lin et al., 2023), originate primarily from natural combustion and anthropogenic emissions (Zhou et al., 2023). These pollutants tend to accumulate in aquatic sediments, where their total concentrations can range from 0.159 to 33090 ng/g (Du and Jing, 2018). Existing research (Sun et al., 2021) has indicated that the ecological risks posed by these substances to aquatic organisms in urban rivers and lakes may be higher than those posed by chlorinated hydrocarbon pollutants (Van Metre and Mahler, 2005), and they have been detected in various ecosystems (Zhang et al., 2021). PAHs are potent carcinogens; both short-term and long-term exposure to them can pose health risks to humans, causing damage to the immune, reproductive, haematopoietic and nervous systems(Premnath et al., 2021; Wu et al., 2011), thereby threatening overall human health. The US Environmental Protection Agency (USEPA) has included 16 PAHs on its list of priority toxic organic pollutants (Ghosal et al., 2016). Among these, benzo[a]pyrene (BaP), due to its tendency to bioaccumulate and its widespread contamination, is often regarded as representative of PAH pollution and its carcinogenic effects (Cai et al., 2019; Revitt et al., 2014); consequently, effective methods for the removal of BaP are attracting increasing attention (Li et al., 2024).

Due to its large surface area and abundant surface functional groups (Chen et al., 2018), biochar has attracted widespread attention in the field of organic pollution treatment in water bodies (Cai et al., 2021; Tian et al., 2020); for example, Yuan et al., (2025) demonstrated that a polishing column constructed using biochar and granular activated carbon(GAC) could effectively adsorb and remove 98.2% and 99.8% of dissolved PAHs from rainwater. However, commercial activated carbon is predominantly produced from raw materials such as coal and wood, and suffers from drawbacks including high costs and limited applications (Bai et al., 2023). Consequently, the development of low-cost adsorbents to replace activated carbon has become a key focus of current research (Bagheri and Abedi, 2009). In recent years, rice straw, owing to its abundant supply and low cost, has emerged as an excellent option for the resource recovery of solid waste (Yang et al., 2021) and is frequently used to produce biochar; however, raw rice straw biochar suffers from issues such as limited adsorption capacity, insufficient active sites and a lack of selectivity towards specific pollutants (Chai et al., 2025)

Researchers have developed various modification strategies to enhance its application efficacy (Cha et al., 2021; Wang et al., 2025), and existing studies have shown that activated biochar, with its porous structure and high specific surface area, can address the above issues and facilitate the adsorption and removal of BaP from the environment (Wang et al., 2023). Existing research primarily classifies biochar activation methods into three categories: physical activation, chemical activation and combined physical-chemical activation (Ge et al., 2023). Physical activation typically involves treatment with steam or CO_2, whilst common activators used in chemical activation include KOH, $KHCO_3$ and H_3PO_4 (Gao et al., 2020). Compared with physical activation methods, activated biochar prepared through modification with chemical reagents typically exhibits superior activation performance (Fu et al., 2019). Chemical activation has attracted widespread research attention due to its advantages, such as a short reaction cycle

and the ability to create a high specific surface area and a well-developed pore structure (Ding et al., 2023). Among these, potassium hydrogen carbonate ($KHCO_3$) is an ideal natural activator (Wang et al., 2022); through gas escape and volatilisation, it etches the carbon framework to create pores, thereby significantly increasing the specific surface area and micropore volume of biochar, and providing abundant adsorption sites for compounds such as BaP (Guo et al., 2023; Zhang et al., 2024). Furthermore, compared with strongly basic activators, the $KHCO_3$ reaction is milder, less corrosive and safer to operate, and is more in line with the principles of green chemistry (Wu et al., 2024). In addition, $KHCO_3$ promotes the aromatisation of the carbon framework, enhancing π-π electron donor–acceptor(EDA) interactions, thereby increasing the adsorption affinity for BaP (Qiu et al., 2022). Previous studies have reported that potassium bicarbonate-modified biochar can be used for the adsorption and removal of methylene blue(Ying et al., 2021), BaP in soil(Wang et al., 2023), and tetracycline in water(Zhang et al., 2026); however, there is still relatively little research on the effect of pyrolysis temperature on the adsorption of BaP by $KHCO_3$-modified biochar and in aquatic environments.

Pyrolysis temperature is a key factor in regulating the physicochemical properties of biochar, directly influencing its yield and material characteristics (Ding et al., 2016) Previous studies have shown that increasing the temperature reduces biochar yield and decreases the number of surface oxygen-containing functional groups with negative charge; the removal of hydrogen and oxygen elements can promote the development of pore structures (Keiluweit et al., 2010). Low-temperature pyrolysis biochar has a lower specific surface area but is rich in oxygen-containing functional groups. At present, further research is required to investigate the effect of different pyrolysis temperatures on the adsorption properties of potassium bicarbonate-modified biochar.

In this study, rice straw was selected as the feedstock to prepare raw biochar via a co-pyrolysis

process; $KHCO_3$ was used as a modifying agent to optimise the biochar's adsorption capacity for BaP. The study systematically investigated the application potential of $KHCO_3$-modified biochar in removing BaP from water at different pyrolysis temperatures. Batch adsorption experiments combined with the response surface method(RSM) were employed to clarify the influence of environmental factors on the adsorption process; differences in the physicochemical characterisation of the biochar before and after modification were compared to elucidate the adsorption mechanism of BaP by the material. The results indicate that rice straw biochar modified with $KHCO_3$ at high temperatures can effectively adsorb BaP from water, providing a theoretical basis for the development of remediation technologies for polycyclic aromatic hydrocarbon pollution in aquatic environments.

2 Materials and Methods

2.1 Reagents and Materials

Hydrochloric acid (HCl, 36%) and potassium bicarbonate ($KHCO_3$, 99.5%) were purchased from Sinopharm Chemical Reagents Co., Ltd.; 3,4-benzopyrene ($C_{20}H_{12}$, 96%) was purchased from McLean Biotechnology; acetonitrile (C_2H_3N, 99.95%) was purchased from Thermo Fisher Scientific; Rice straw. Deionised water was used in all experiments.

2.2 Biochar Production

Preparation of biochar from rice straw: Straw powder sieved through a 100-mesh sieve was placed in a covered ceramic crucible and pyrolysed in a muffle furnace at a heating rate of 5 ℃/min up to 800℃ for 1 hour; after cooling, the black product was washed with 0.1 mol/L HCl and rinsed with water until neutral, then dried in an oven at 80℃ for 24 hours and ground to a fineness of 100 mesh to obtain BC. Co-pyrolysis modification was carried out by mixing straw powder with $KHCO_3$ in a 1:1 mass ratio and

grinding for 30 minutes. A feed rate of 10 g was used, and pyrolysis was conducted for 1 hour at 700, 800 and 900℃, respectively, at the same heating rate. The subsequent acid washing, water washing, drying and sieving steps were identical to those in the BC preparation process; the resulting modified biochar were named PBC700, PBC800 and PBC900 respectively.

2.3 Adsorption experiments

Weigh out BaP powder and dissolve it in acetonitrile to prepare BaP stock solutions of varying concentrations; then prepare the BaP solutions required for the test using a mixture of acetonitrile and water in a ratio of 10:90.

Weigh out 10.0 mg of each of the four types of biochar and place them separately into 50 mL brown centrifuge tubes. Add 30 mL of a BaP solution with a concentration of 20 mg/L and pH 7.0, and placed in a constant-temperature shaker at 25℃ and 180 r/min for 72 hours. Samples of 1 mL were taken at regular intervals, mixed thoroughly with 4 mL of acetonitrile, and filtered through a 0.22 μm nylon filter membrane; At the same time, the additional loss of BaP is corrected by setting adsorbent blanks and solvent blanks. The filtrate was transferred to a 2 mL chromatography vial and analysed by HPLC (Agilent 1260). For details on adsorption kinetics (Text S1), adsorption isotherms (Text S2) and adsorption thermodynamics (Text S3), see the supplementary information.

2.4 Methods for the detection of BaP

The method for the determination of BaP is based on ‘High-Performance Liquid Chromatography for the Determination of Benzo[a]pyrene in Soil’ (DB53/T 704-2015). The specific analytical conditions are as follows: The chromatographic column is a C18 column (250 mm × 4.6 mm) with a particle size of 5 μm. The mobile phase consists of acetonitrile:water (V/V) = 75 : 25, with a flow rate of 1.0 mL/min.

The column temperature is 30 ± 1 °C, the detection wavelength is 430 nm, the excitation wavelength is 290 nm, and the injection volume is 10 μL.

2.5 Material characterisation

The infrared spectra of four types of biochar in the range of 400-4000 cm^{-1} were recorded using a Fourier transform infrared spectrometer (FTIR) (Bruker, Germany, VERTEX 70), with 64 scans over a period of 42 s.; surface morphology data were obtained using a scanning electron microscope (SEM) from China Chuangpu (SU8600); The samples were degassed under vacuum at 120℃ for 8 hours; the adsorption-desorption curves were then measured at 77 K using high-purity nitrogen as the adsorbent to calculate the specific surface area (Brunauer-Emmett-Teller method), total pore volume and mean pore diameter (Barrett-Joyner-Halenda method), and micropore volume (t-Plot method). X-ray diffraction (XRD) was used to determine the composition of the biochar within a scanning range of 5°to 85°,Scan speed: 10 °/min, step size: 0.02°(Bruker Corporation, USA, D8 ADVANCE).

2.6 Data Analysis

The experimental data were processed and plotted using Excel 2019 and Origin 2024 statistical analysis software. Data processing and tests for significance were carried out using SPSS 26; Box-Behnken design and response surface analysis were performed using Design-Expert 13.

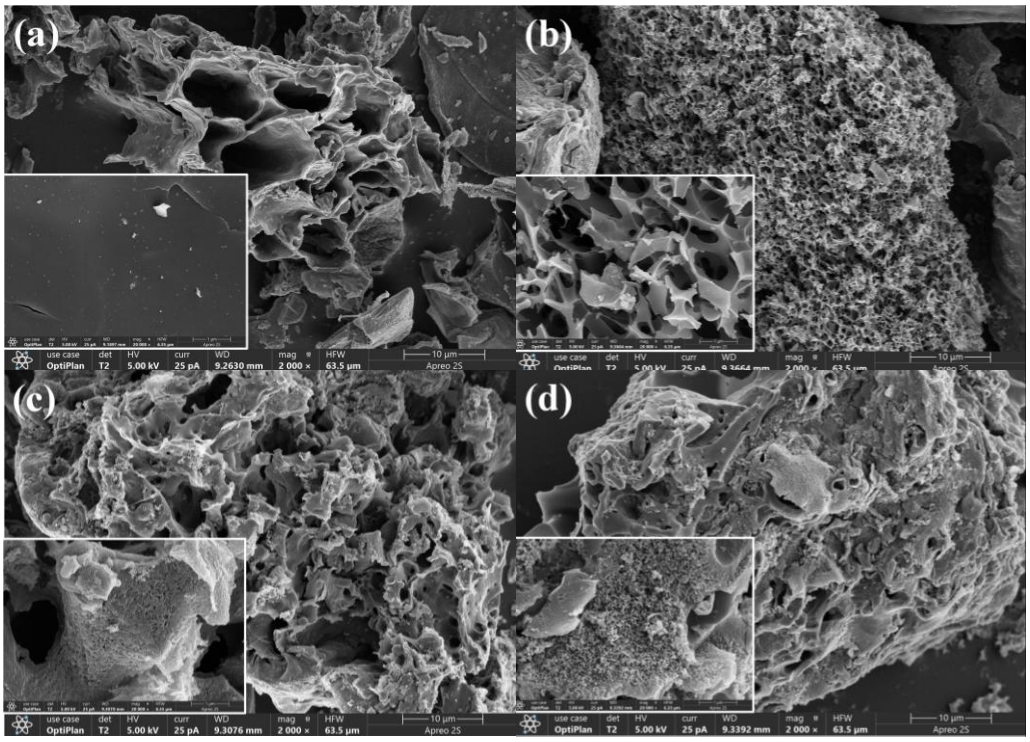


Fig.1 Scanning electron microscope images of biochar: (a) BC, (b) PBC700, (c) PBC800, (d) PBC900

3 Results and discussion

3.1 Characterization of the biochars

An analysis of the microscopic surface topography of the four materials revealed that the smooth surface of BC was significantly etched following modification with $KHCO_3$ (Fig. 1), with the appearance of numerous irregular pits and fissures and the initial development of pores. As the pyrolysis temperature increased, the activating effect of $KHCO_3$ intensified, leading to an increase in the number of surface pores and more regular pore channels. This is because the gases generated by the pyrolysis of $KHCO_3$ continuously impacted the biochar surface, exacerbating the surface roughness of the material; The K_2CO_3 generated during pyrolysis penetrates the cellulose component of the biomass, weakening the intermolecular hydrogen bonds within the rice straw and disrupting the original structure of the biomass,

thereby promoting the development of micropores. When the pyrolysis temperature reaches 700-800℃, potassium reacts with carbon to form metallic potassium, which further etches the carbon matrix (Obanla et al., 2023). Metallic potassium vapour becomes embedded between the carbon layers, driving the activation process and ultimately forming a coral-like, spherical, three-dimensional, multi-level pore structure, which significantly enhances the pore structure of the biochar (Huang et al., 2018). The N_2 adsorption capacities of the four biochar samples followed the order PBC900> PBC800> PBC700> BC (Fig. S1). Following $KHCO_3$ modification, the N_2 adsorption-desorption isotherms shifted from Type III to a composite of Type I and Type IV characteristics, with increased adsorption in the low-pressure region, a mesoporous peak appeared in the BJH pore size distribution. As the pyrolysis temperature was increased, both the isotherm adsorption capacity and the peak value of the BJH mesoporous distribution for the biochar further increased. This indicates that high-temperature pyrolysis activation followed by $KHCO_3$ modification can increase the specific surface area and total pore volume of the biochar, forming a greater number of micropores and reducing the average pore diameter (Gan et al., 2021) (Table S1). This is consistent with the studies by Wei et al., (2023) and Zhang et al., (2022), thereby providing more active sites for pollutant removal.

FTIR analysis revealed absorption peaks at 1568.8 cm^{-1} (aromatic C=C), 1096.0 cm^{-1} (C-O-C, C-O), 798.9 cm^{-1} (C-H) and 473.1 cm^{-1} (O-Si-O) (Fig. 2a). This indicates that $KHCO_3$ modification at high temperatures promotes the evolution of the carbon skeleton towards a more aromatic structure (Deng et al., 2024), with the surface tending towards a more hydrophobic and more aromatic carbon structure. This is consistent with the findings of Ding et al., who concluded that adsorption parameters exhibit a linear relationship with the aromaticity and total surface area of the adsorbent, and increase with rising pyrolysis temperature (Ding et al., 2018). XRD analysis revealed two broad diffraction peaks at 22.3°

and 43.8° in the biochar (Fig. 2b), corresponding to amorphous carbon (002) and crystalline/ graphitic carbon (101). At high temperatures, $KHCO_3$ modification causes a slight shift or broadening of the graphitic orientation and microcrystalline size, enhancing the reorganisation of the carbon structure, shifting it towards an amorphous state and thereby strengthening the biochar's affinity for pollutants (Jiang et al., 2022).

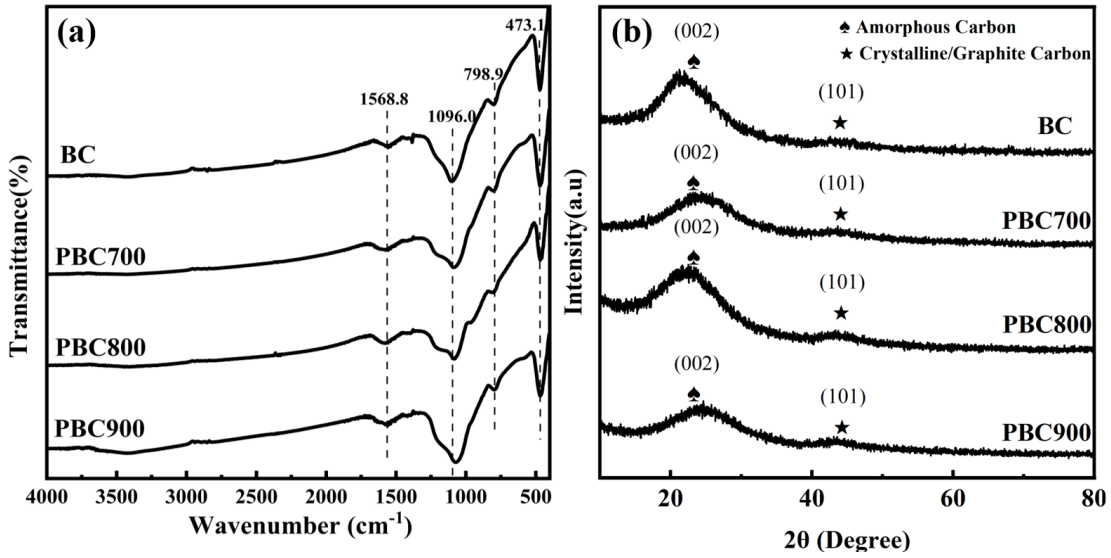


Fig. 2 Infrared spectra (a) and X-ray diffraction patterns (b) of the four types of biochar

3.2 Adsorption of BaP by modified biochar

The adsorption of BaP by the four types of biochar is shown in (Fig. 3a). The removal efficiencies of BaP by PBC900, PBC800, PBC700 and BC were 81.59%, 79.30%, 55.69% and 42.74%, respectively. In comparison, modification with $KHCO_3$ enhanced the adsorption of BaP by biochar; this enhancement effect increased progressively with rising pyrolysis temperature, although the difference in modification efficacy between the 800℃ and 900℃ conditions was limited. Taking into account both energy consumption and activation efficacy, 800℃ is a relatively economical and suitable pyrolysis temperature.

Using the established method described in Text S4, the adsorption kinetics curves of the four biochars were fitted; Table 1 shows that PBC exhibited the highest goodness of fit with the pseudo-

second-order model, This indicates that modified biochar exhibits a certain degree of chemical adsorption. The adsorption of BaP involves chemical mechanisms such as electron exchange and complexation (Lu et al., 2025), whilst BC showed the best fit with the pseudo-first-order model, indicating that the adsorption of BaP by BC is primarily due to simple diffusion, which is consistent with the findings of Barman et al., (2021). Furthermore, the goodness of fit increases with rising pyrolysis temperature, suggesting that the adsorption mechanism of biochar evolves from a partitioning advantage at low pyrolysis temperatures to an adsorption advantage at high pyrolysis temperatures.

Table 1 Fitting parameters of adsorption kinetic models for BaP by biochars

Kinetics models	Parameters	BC	PBC700	PBC800	PBC900
Pseudo-first-order kinetic model	Q_e	24.59	31.49	46.24	47.49
	K_1	0.00228	0.00253	0.00928	0.00945
	R^2	0.9981	0.9838	0.9276	0.9269
Pseudo-Second-Order Kinetic Model	Q_e	27.54	35.06	48.01	49.41
	K_1	0.096	0.102	0.361	0.353
	R^2	0.9964	0.9978	0.9996	0.9997
Elovich Model	Q_e	0.118	0.200	3.257	3.434
	K_1	0.161	0.136	0.147	0.143
	R^2	0.9692	0.9861	0.9307	0.9348

Judging from the fitting results, PBC800 exhibited the highest adsorption rate constant K_2 (Fig. 3b, 0.361 mg/mg/min), whilst PBC900 was second only to PBC800 at 0.353 mg/mg/min; The A values for PBC900 and PBC800 in the Elovich model were significantly higher than those for PBC700 and BC, indicating that high-temperature $KHCO_3$ modification can enhance the affinity of biochar for BaP, consistent with the findings of Wang et al., (2023); As the pyrolysis temperature increased, the equilibrium adsorption capacity of biochar for BaP increases accordingly, suggesting that $KHCO_3$ modification enhances the specific surface area of biochar and alters its surface functional groups, thereby improving its adsorption performance (Qiu et al., 2009).

As shown in Fig. S2, the intraparticle diffusion model divides the adsorption process into three stages (Kleemann et al., 2025). Adsorption onto surface vacancies within the 0-4 hours is the most

efficient stage; during this period, the K_1 values for PBC900 and PBC800 are positive, whilst those for PBC700 and BC are negative. This indicates that high-temperature modification has enriched the active sites on the biochar surface, thereby enhancing its adsorption capacity for BaP. The period from 4 to 24 h constitutes the second stage, during which BaP overcomes the energy barrier to diffuse into internal sites within the pores and interlayer spaces. After 24 h, the system enters the third stage of adsorption saturation. In this stage, the slope is greater than 0, indicating stable adsorption; no desorption occurs after equilibrium is reached. The curve fitted by this model does not pass through the origin, suggesting that the BaP adsorption rate is jointly governed by the dual mechanisms of surface adsorption and intraparticle diffusion.

Table 2 Fitting parameters of the intraparticle diffusion model for BaP by biochars

Parameters	BC	PBC700	PBC800	PBC900
K_{P1}	0.740	1.174	1.911	1.956
C_1	-2.11	-2.64	5.98	6.34
R_1^2	0.9658	0.9383	0.9295	0.9387
K_{P2}	0.295	0.416	0.075	0.090
C_2	11.22	12.18	43.83	44.56
R_2^2	0.9064	0.9804	0.8453	0.8050
K_{P3}	0.020	0.007	0.022	0.017
C_3	23.52	32.26	45.83	47.52
R_3^2	0.9440	0.9448	0.9999	0.9932

The isotherm adsorption curves were fitted using the Langmuir, Freundlich, Temkin and D-R models; the fitting methods are detailed in Text S5. All models provided a good fit to the experimental data (Table 2), with the Langmuir model yielding the highest R^2 value, indicating that the adsorption process is monolayer adsorption (Yu et al., 2009). The equilibrium adsorption capacities of BaP for all four biochar types showed a trend of initially rapid increase followed by approaching saturation (Fig. 3c), with the increase being more pronounced for the high-temperature-modified biochar. The Q_m values for BaP for the four biochar types were PBC900 (54.70 mg/g), PBC800 (55.41 mg/g), PBC700 (38.70 mg/g) and BC (25.47 mg/g), which are close to the measured equilibrium adsorption capacities. The PBC900

has a higher BET specific surface area and a higher BaP adsorption capacity; however, high-temperature activation produces a large amount of N_2, which occupies micropores that are difficult for BaP to penetrate, resulting in fewer effective adsorption sites. Consequently, the resulting Q_m value is lower than that of the PBC800.

PBC800 exhibited a significantly higher adsorption capacity for BaP than BC. The non-linear coefficient N in the Freundlich model ranged from 0.30 to 0.45, all of which were less than 1, indicating that the adsorption isotherms followed an L-type profile and that the adsorption processes proceeded spontaneously. As the pyrolysis temperature increased, the value of N decreased, suggesting that higher pyrolysis temperatures enhanced the affinity of PBC for BaP (Zhu et al., 2018), thereby increasing the adsorption capacity; Meanwhile, the fitting results from the Temkin and D-R models show that as modification and pyrolysis temperature increase, the value of b gradually decreases, whilst the Q_S value gradually increases, indicating that high-temperature modification can enhance the adsorption of BaP by biochar and the maximum micropore filling capacity of the biochar. The E values of all four biochars are less than 8 kJ/mol, suggesting that the adsorption of BaP by biochar is dominated by physical interactions (Simsek et al., 2022), involving strong physical binding mechanisms such as π-π interactions and hydrophobic adsorption.

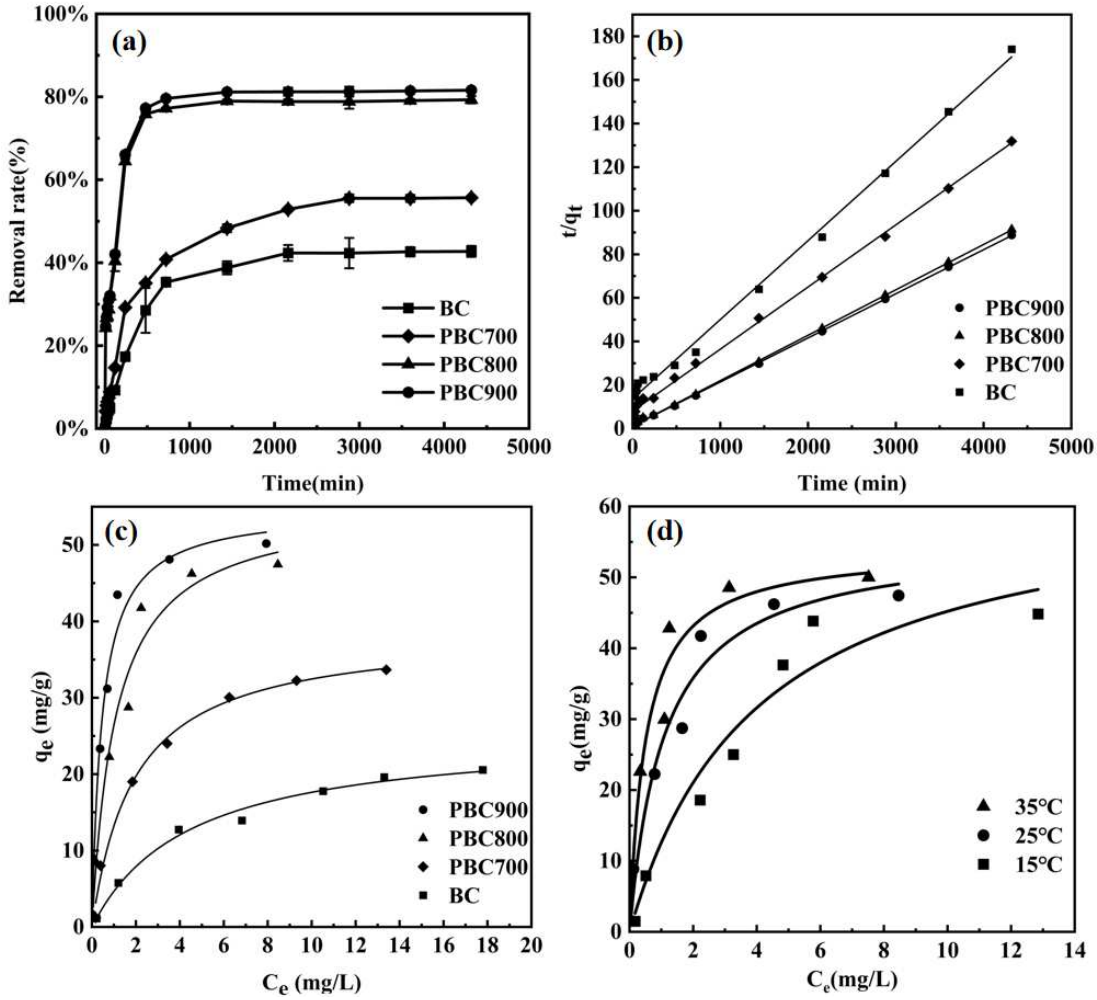


Fig.3 Experiments on the adsorption of BaP from water by biochar: (a) Adsorption of BaP by different types of biochar; (b) Pseudo-second-order kinetic model; (c) Langmuir isotherm model; (d) Langmuir model fit for BaP adsorption by PBC800 at different temperatures

Adsorption thermodynamic experiments were conducted on four types of biochar at 15, 25 and 35℃ (Fig. 3d). As the temperature increased, the equilibrium adsorption capacity of the biochar for BaP increased, indicating that the process is an endothermic reaction. This positive temperature effect stems from the endothermic nature of BaP desolvation and the activation diffusion within the micropores. Increased temperature reduces solution viscosity and intensifies molecular thermal motion, which facilitates the disruption of hydration structures and the overcoming of diffusion energy barriers, whilst simultaneously exposing hydrophobic sites on the biochar and enhancing π-π stacking interactions. This

results in a synergistic thermodynamic and kinetic increase in BaP adsorption capacity (Kronberg, 2016). The equilibrium constant K_L and 1/T obtained from the Langmuir model fit were linearly fitted using the van't Hoff equation (Text S6); the fitted curve showed an $R^2 > 0.85$, indicating a good linear relationship (Fig. S3). For all four biochar types, ΔG was negative and ΔH was positive at different temperatures (Table S2), indicating that the adsorption process is an endothermic reaction and that spontaneous adsorption occurs (Gupta and Singh, 2018). Consistent with the adsorption thermodynamic experiments, as $KHCO_3$ modification and pyrolysis temperature increased, the absolute values of ΔG, ΔH and ΔS increased in that order (BC< PBC700< PBC800< PBC900). This suggests that modification and high-temperature pyrolysis synergistically enhance the adsorption affinity of biochar for BaP; this trend is consistent with the changes in specific surface area and micropore volume. Whilst a well-developed micropore structure enhances adsorption capacity, it also requires the overcoming of a higher energy barrier for adsorption.

3.3 The Effect of Operating Parameters on the Adsorption of BaP from Water by PBC800

As shown in Fig. 4a, within the experimental pH range, the adsorption capacity increases as the pH decreases (Gupta and Singh, 2018), this may be attributed to the increased protonation of oxygen-containing functional groups (such as carboxyl and phenolic hydroxyl groups) on the surface of PBC800 under low pH conditions (Jang and Kan, 2019), which enhances the surface positive charge whilst reducing the competitive adsorption of water molecules, thereby strengthening the π-π stacking and hydrophobic interactions between the aromatic structures of the biochar and BaP.

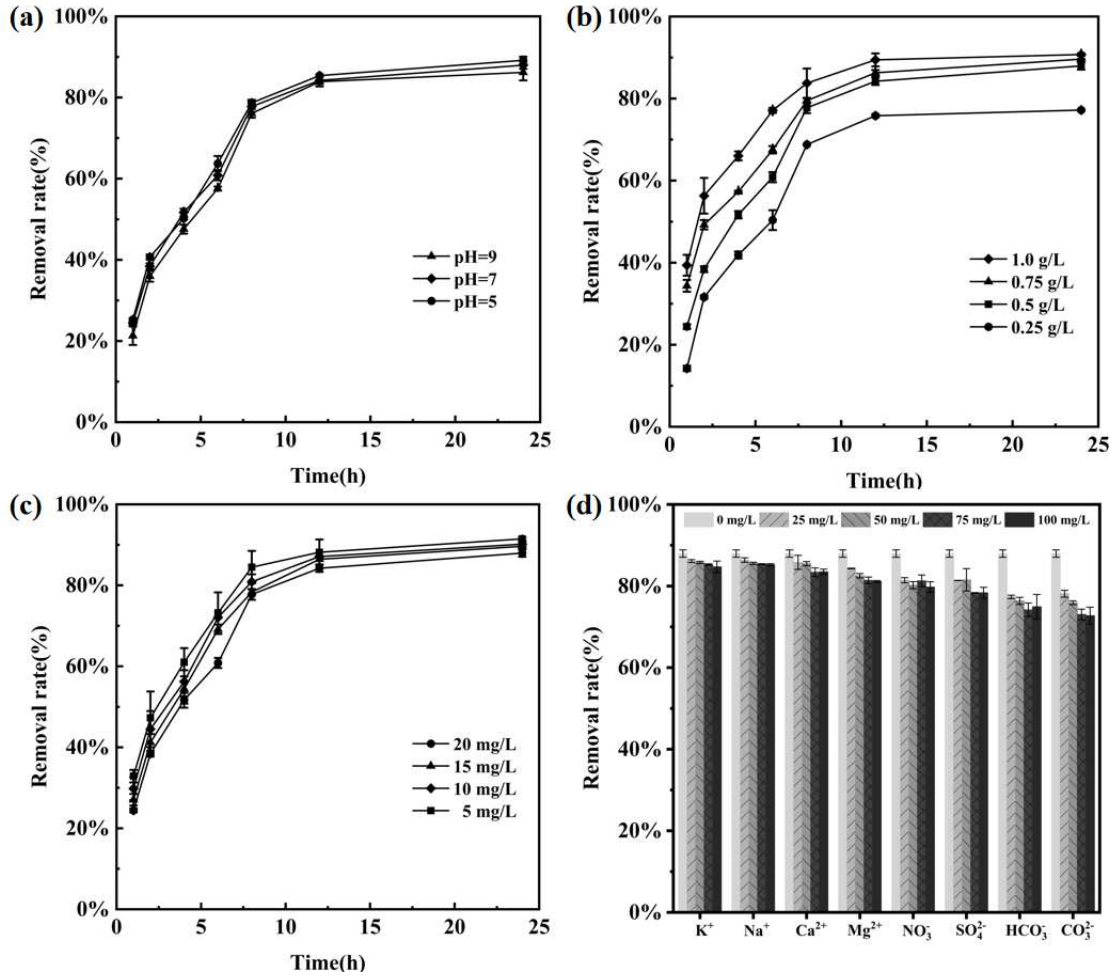


Fig. 4 Effect of operational parameters on the adsorption of BaP from water by PBC800: (a) initial reaction pH (temperature=35°C, PBC800=1 g/L, BaP=20 mg/L); (b) PBC800 dosage (temperature=35°C, pH=5, BaP=20 mg/L); (c) BaP concentration (temperature=35°C, PBC800=1 g/L, pH=5); (d) ions in the aqueous solution (temperature=35°C, PBC800=1 g/L, BaP=20 mg/L, pH=5)

The dosage of PBC800 had a significant effect on BaP adsorption (Fig. 4b); as the dosage increased from 0.25 g/L to 1.0 g/L, both the adsorption rate and the equilibrium removal efficiency increased significantly. This is because a higher dosage of biochar provides more adsorption sites and a larger specific surface area, thereby enhancing the opportunities for BaP to come into contact with the biochar surface (Liu et al., 2024). However, the adsorption capacity per unit of adsorbent showed a decreasing trend as the dosage increased. This is attributed to adsorbent agglomeration at high dosages, reduced

utilisation of effective specific surface area, and relatively insufficient adsorbate concentration (Ilyas et al., 2021). Taking into account both removal efficiency and the cost-effectiveness of the adsorbent, 0.75 g/L is the optimal dosage.

PBC800 exhibits some variation in adsorption behaviour at different initial BaP concentrations (Fig. 4c). As the BaP concentration decreases, the removal efficiency increases; at low concentrations, there are ample adsorption sites on the biochar, enabling efficient capture of BaP. As the initial concentration rises, the active sites tend to become saturated, leading to a decrease in the removal rate (Minkina et al., 2022). It takes longer to reach equilibrium in high-concentration systems, reflecting the effects of concentration-gradient-driven mass transfer and site competition (Sambo et al., 2024). This result is consistent with the characteristics of monolayer adsorption and limited sites described by the Langmuir isotherm model, further confirming that the adsorption of BaP by PBC800 is dominated by the number of active sites on the surface (Li et al., 2022).

The presence of different ions exerted an inhibitory effect on the adsorption of BaP by PBC800 (Fig. 4d). We first investigated the influence of different cations on BaP adsorption and found that Mg^{2+} exhibited the most pronounced inhibitory effect, followed by Ca^{2+} and K^{+}, whilst Na^{+} had the weakest inhibitory effect. Specifically, divalent cations exerted a greater inhibitory effect on adsorption than monovalent cations; Among the anions, CO_3^{2-} and HCO_3^{-} exhibited the most significant inhibitory effects, with removal efficiencies decreasing from 87.96% to 72.73% and 74.92% respectively, whilst the reduction in removal efficiency for NO_3^{-} and SO_4^{2-} was relatively minor. Overall, the inhibitory effect increases with rising concentration; High concentration ions compete with BaP for adsorption sites, whilst cations have a lesser impact; in actual aquatic environments, greater attention should be paid to the influence of carbonate anions. The overall removal rate remained at a high level, indicating that

$KHCO_3$-modified biochar can adapt to complex aquatic environments; this is primarily attributed to pore filling and π-π electron donor-acceptor (EDA) interactions being the main mechanisms of BaP adsorption (Wang et al., 2023).

3.4 Response surface analysis of BaP adsorption by PBC800 in aqueous solutions

The results of the Box-Behnken Design (BBD) are presented in Table S3. The probability plot of residuals (Fig. S4a) shows that the model residuals follow a normal distribution; the statistical assumptions for the constructed Box-Behnken response surface model are satisfied, and the model is reliable. The scatter plot of measured and predicted values lies closely along the line y=x (Fig. S4b), indicating that the model fits the data well. The analysis of variance in Tables S4 and S5 indicates that the quadratic response surface model is highly significant ($p< 0.01$), with R^2=0.9664; the difference between the adjusted coefficient of determination and R^2 is less than 0.2, suggesting that the model effectively explains the interactions between factors and that the variables were selected appropriately. The test for non-conformity to the model showed no significant deviation ($p> 0.05$); the coefficient of variation (CV) was 2.75%, and the signal-to-noise ratio was 14.97, which is well above the reasonable threshold. This demonstrates good experimental precision and model reliability; the response surface model exhibits excellent fitting and predictive performance and can accurately characterise the interactions between environmental factors and the adsorption of BaP by biochar. The initial concentration of BaP, the amount of biochar added and the temperature all significantly influenced the adsorption efficiency ($p< 0.05$), consistent with the conclusions of the single-factor experiments, indicating that this model can identify the optimal parameters for the adsorption of BaP from water by PBC800. Based on this, a functional relationship between the environmental factors and the response

variable was established using a multiple quadratic regression equation (Text S7).

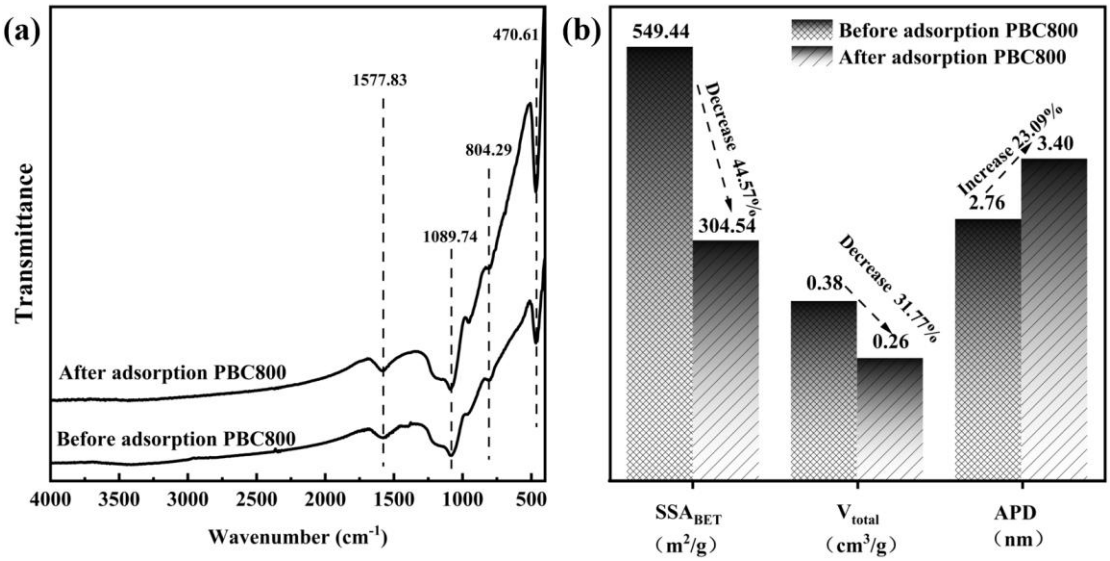
The response surface results (Fig. S5) show that the steepness of the response surface provides an intuitive indication of the strength of the influence of each factor on BaP removal efficiency: the steeper the surface gradient, the more significant the fluctuations in degradation efficiency caused by changes in that factor, i.e. the greater the influence of that factor (Tangsiri and Nezamzadeh-Ejhieh, 2020)Contour plots can be used to determine the significance level of interactions between factors; if the contours are elliptical, this indicates a significant interaction between the two factors; if the contours approach a circular shape, the interaction is weaker (Puri et al., 2021). Reducing the initial BaP concentration and increasing the PBC dosage are conducive to improving the removal rate, with the effect of PBC dosage being greater than that of the initial concentration; both increasing the temperature and the PBC dosage can increase the removal rate, but the rate of increase slows at high dosages, and the effect of PBC dosage is stronger than that of temperature. The interaction between the initial BaP concentration and temperature is weak, with linear main effects predominating; the removal rate decreases as the initial concentration rises and increases as the temperature rises, with temperature having a greater influence than the initial concentration. The optimal conditions are a low pollutant concentration and a relatively high temperature. Based on the characteristics of the surface gradient, the order of factor influence from strongest to weakest is PBC dosage> temperature> initial BaP concentration, which is consistent with the pattern obtained from the F-value of the analysis of variance. Substituting the boundary conditions (initial BaP concentration of 10 mg/L, PBC dosage of 15 mg, and temperature of 35°C) into the quadratic regression model yields a predicted BaP removal rate of 94.08% under these conditions. As the theoretical extreme point of the model exceeds the upper limit of the experimental temperature range, these conditions represent the optimal predicted operating conditions within the range defined for this

experiment.

3.5 Adsorption Mechanism of BaP by Modified Biochar

A comparison of the infrared spectra and pore structure parameters of PBC800 before and after BaP adsorption reveals that the characteristic aromatic peaks at 1577 cm^{-1} and 804 cm^{-1} shifted to the blue after adsorption (Fig. 5a). This may be due to the close stacking of BaP with the aromatic layer of the biochar, which restricts the out-of-plane vibration of the C-H bonds (Ahmed et al., 2018; Chen et al., 2025), resulting in an increase in frequency, or because BaP forms π-π stacking with the biochar's aromatic structure (Wang et al., 2023), altering the electron cloud distribution and bonding interactions within the aromatic rings; The red shift of the characteristic peak at 470 cm^{-1} may be attributed to increased rigidity in the aromatic stacking system, leading to a decrease in vibrational frequency.

Following adsorption, the specific surface area of PBC800 decreased from 549.44 m^2/g to 304.54 m^2/g, a reduction of 44.6%; the total pore volume decreased from 0.38 cm^3/g to 0.26 cm^3/g, a reduction of 31.6 % (Fig. 5b). This indicates that BaP was successfully adsorbed within the pore network of the biochar, preventing nitrogen gas from entering the filled pores. Meanwhile, the average pore diameter increased from 2.76 to 3.4 nm, a rise of 23.2%, suggesting that BaP filled and blocked the micropores, resulting in an overall overestimation of the pore diameter. The evolution of the pore structure before and after adsorption indicates that BaP preferentially fills the micropores of the biochar rather than adsorbing onto its external surface, confirming that pore filling is a key adsorption mechanism (Cheng et al., 2020; Quach An and Kajitvichyanukul, 2019). PBC800, obtained by pyrolysis at 800℃ following $KHCO_3$ modification, is rich in micropores and can effectively capture BaP, whilst retaining a large number of active adsorption sites after adsorption.



371

372 **Fig. 5** Infrared spectra of PBC800 before and after BaP adsorption (a) and changes in specific surface

373 area and porosity (b)

374 **4 Conclusion**

375 This study utilised rice straw as raw material to prepare biochar through co-pyrolysis with $KHCO_3$,

376 for use in the adsorption and remediation of BaP in water bodies. High-temperature etching with $KHCO_3$

377 enriches the material's microporous structure and enhances its degree of aromatisation. PBC800,

378 prepared via $KHCO_3$ modification at 800℃, exhibited the best overall performance, showing the closest

379 fit to the pseudo-second-order kinetics and the Langmuir model, with a saturation adsorption capacity of

380 55.41 mg/g. Response surface analysis indicates that the factors influence the process in the following

381 order of strength: biochar dosage> temperature> initial BaP concentration. Under optimal conditions, the

382 theoretical removal rate is 94.08%; however, the interference of carbonate ions should be taken into

383 account during the actual adsorption process. The adsorption process is predominantly spontaneous,

384 endothermic physical adsorption, accompanied by a composite adsorption process involving weak π-π

385 electron donor-acceptor interactions, with microporous filling and π-π stacking as the core mechanisms.

Author Contributions Yang Yin, Yun Yang: Conceptualization. Yun Yang: methodology, validation and formal analysis. Yun Yang, Qian Liu: software. Hongqing Hu, Yun Yang: investigation. Yonghong Liu, Qingling Fu: resources. Qian Liu: data curation, supervision, writing-original draft preparation, writing-review & editing. Jun Zhu, Yonghong Liu, Hongqing Hu: visualization. Hongqing Hu: project administration, funding acquisition. All authors have read and agreed to the published version of the manuscript.

Funding Funded by the National Key Research and Development Programme under the 14th Five-Year Plan (2023YFC3709804).

Data Availability Data are available upon request from the authors.

Declarations We declare that accepted principles of ethical and professional conduct have been followed.

Conflicts of Interest The author declares that there are no conflicts of interest in this research.

References

Ahmed, M. B., Zhou, J. L., Ngo, H. H., Johir, M. A. H., Sun, L., Asadullah, M. & Belhaj, D.: 2018, Sorption of hydrophobic organic contaminants on functionalized biochar: Protagonist role of π-π electron-donor-acceptor interactions and hydrogen bonds. *Journal of Hazardous Materials*, *360*, 270-278. https://doi.org/.10.1016/j.jhazmat.2018.08.005

Bagheri, N. & Abedi, J.: 2009, Preparation of high surface area activated carbon from corn by chemical activation using potassium hydroxide. *Chemical Engineering Research & Design*, *87*, 1059-1064. https://doi.org/.10.1016/j.cherd.2009.02.00

Bai, X. L., Quan, B. Y., Kang, C. Y., Zhang, X. L., Zheng, Y., Song, J., Xia, T. & Wang, M.: 2023, Activated carbon from tea residue as efficient absorbents for environmental pollutant removal from wastewater. *Biomass Conversion and Biorefinery*, *13*, 13433-13442. https://doi.org/.10.1007/s13399-022-02316-4

Barman, S. R., Das, P. & Mukhopadhayay, A.: 2021, Biochar from waste Sterculia foetida and its application as adsorbent for the treatment of PAH compounds: Batch and optimization. *Fuel*, *306*. https://doi.org/.10.1016/j.fuel.2021.12162

Cai, S., Zhang, Q., Wang, Z. Q., Hua, S., Ding, D. H., Cai, T. M. & Zhang, R. H.: 2021, Pyrrolic N-rich biochar without exogenous nitrogen doping as a functional material for bisphenol A removal: Performance and mechanism. *Applied Catalysis B-Environment and Energy*, *291*. https://doi.org/.10.1016/j.apcatb.2021.12009

Cai, T., Ding, Y., Zhang, Z., Wang, X., Wang, T., Ren, Y. & Dong, Y.: 2019, Effects of total organic carbon content and leaching water volume on migration behavior of polycyclic aromatic hydrocarbons in soils by column leaching tests. *Environmental Pollution*, *254*. https://doi.org/.10.1016/j.envpol.2019.11298

Cha, J. S., Jang, S.-H., Lam, S. S., Kim, H., Kim, Y.-M., Jeon, B.-H. & Park, Y.-K.: 2021, Performance of CO2 and Fe-modified lignin char on arsenic (V) removal from water. *Chemosphere*, *279*. https://doi.org/.10.1016/j.chemosphere.2021.13052

Chai, W. S., Aslam, A. A., Li, X. Y., Wu, T. & Pang, C. H.: 2025, Surface-engineered biochar: Recent advances in modification strategies for environmental remediation and energy applications. *Journal of Environmental Chemical Engineering*, *13*. https://doi.org/.10.1016/j.jece.2025.117951

Chen, L. W., Yang, S. J., Zuo, X., Huang, Y., Cai, T. M. & Ding, D. H.: 2018, Biochar modification significantly promotes the activity of Co3O4 towards heterogeneous activation of peroxymonosulfate. *Chemical Engineering Journal*, *354*, 856-865. https://doi.org/.10.1016/j.cej.2018.08.09

Chen, Q., Feng, H., Dong, J., Huang, Y., Yi, P., Wu, M. & Pan, B.: 2025, Enhancing insight into sorption-degradation interplay: A comparative study on the removal of organics by biochar through experiments and theoretical calculations. *Separation and Purification Technology*, *354*. https://doi.org/.10.1016/j.seppur.2024.12851

Cheng, H., Ji, R., Bian, Y., Jiang, X. & Song, Y.: 2020, From macroalgae to porous graphitized nitrogen-doped biochars - Using aquatic biota to treat polycyclic aromatic hydrocarbons-contaminated water. *Bioresource Technology*, *303*. https://doi.org/.10.1016/j.biortech.2020.122947

Deng, Y., Chen, J., Xiao, Z., Liu, J., Zhang, J., Zhu, B., You, X., Ni, F., Ao, T. & Tan, Y.: 2024, A Novel N Self-Doped Porous Biochar Synthesized by $KHCO_3$-Activated Chicken Feather for the Remediation of Tetracycline-Contaminated Water and Soil. *Water Air and Soil Pollution*, *235*. https://doi.org/.10.1007/s11270-024-06933-9

Ding, E. R., Jiang, J. Q., Lan, Y., Zhang, L. D., Gao, C. X., Jiang, K. X., Qi, X. X. & Fan, X. L.: 2023, Optimizing Cd^{2+} adsorption performance of KOH modified biochar adopting response surface methodology. *Journal of Analytical and Applied Pyrolysis*, *169*. https://doi.org/.10.1016/j.jaap.2022.10578

Ding, Z., Zhang, F., Sun, N., Chi, J. & Iop: 2018, Sorption of polycyclic aromatic hydrocarbons by biochars of wheat straw with different pyrolysis temperatures, 4th International Conference on Advances in Energy Resources and Environment Engineering (ICAESEE). Chengdu, PEOPLES R CHINA. https://doi.org/.10.1088/1755-1315/237/5/052008

Ding, Z. H., Wan, Y. S., Hu, X., Wang, S. S., Zimmerman, A. R. & Gao, B.: 2016, Sorption of lead and methylene blue onto hickory biochars from different pyrolysis temperatures: Importance of physicochemical properties. *Journal of Industrial and Engineering Chemistry*, *37*, 261-267. https://doi.org/.10.1016/j.jiec.2016.03.03

Du, J. J. & Jing, C. Y.: 2018, Anthropogenic PAHs in lake sediments: a literature review (2002-2018). *Environmental Science-Processes & Impacts*, *20*, 1649-1666. https://doi.org/.10.1039/c8em00195

Fu, Y. H., Shen, Y. F., Zhang, Z. D., Ge, X. L. & Chen, M. D.: 2019, Activated bio-chars derived from rice husk via one- and two-step KOH-catalyzed pyrolysis for phenol adsorption. *Science of the Total Environment*, *646*, 1567-1577. https://doi.org/.10.1016/j.scitotenv.2018.07.42

Gan, F., Cheng, B., Jin, Z., Dai, Z., Wang, B., Yang, L. & Jiang, X.: 2021, Hierarchical porous biochar from plant-based biomass through selectively removing lignin carbon from biochar for enhanced removal of toluene. *Chemosphere*, *279*. https://doi.org/.10.1016/j.chemosphere.2021.13051

Gao, Y., Yue, Q. Y., Gao, B. Y. & Li, A. M.: 2020, Insight into activated carbon from different kinds of chemical activating agents: A review. *Science of the Total Environment*, *746*. https://doi.org/.10.1016/j.scitotenv.2020.14109

Ge, Q., Li, P., Liu, M., Xiao, G. M., Xiao, Z. Q., Mao, J. W. & Gai, X. K.: 2023, Removal of methylene blue by porous biochar obtained by KOH activation from bamboo biochar. *Bioresources and Bioprocessing*, *10*. https://doi.org/.10.1186/s40643-023-00671-

Ghosal, D., Ghosh, S., Dutta, T. K. & Ahn, Y.: 2016, Current State of Knowledge in Microbial Degradation of Polycyclic Aromatic Hydrocarbons (PAHs): A Review. *Frontiers in Microbiology*, *7*. https://doi.org/.10.3389/fmicb.2016.0136

Guo, S. J., Zou, Z. Y., Chen, Y., Long, X. X., Liu, M., Li, X. P., Tan, J. H. & Chen, R. Z.: 2023, Synergistic effect of hydrogen bonding and π-π interaction for enhanced adsorption of rhodamine B from water using corn straw biochar?. *Environmental Pollution*, *320*. https://doi.org/.10.1016/j.envpol.2023.12106

Gupta, H. & Singh, S.: 2018, Kinetics and thermodynamics of phenanthrene adsorption from water on orange rind activated carbon. *Environmental Technology & Innovation*, *10*, 208-214. https://doi.org/.10.1016/j.eti.2018.03.00

Huang, Y., Li, K., Yao, W. & Gao, Y.: 2018, Factors affecting the pore structure and adsorption performance of rice straw carbon prepared by potassium bicarbonate activation. *Environ. Chem*, *37*, 569-575.

Ilyas, M., Ahmad, W. & Khan, H.: 2021, Utilization of activated carbon derived from waste plastic for decontamination of polycyclic aromatic hydrocarbons laden wastewater. *Water Science and Technology*, *84*, 609-631. https://doi.org/.10.2166/wst.2021.252

Jang, H. M. & Kan, E.: 2019, A novel hay-derived biochar for removal of tetracyclines in water. *Bioresource Technology*, *274*, 162-172. https://doi.org/.10.1016/j.biortech.2018.11.081

Jiang, J., Ruan, C. J., Chen, X. Y., Wu, Y. & Wang, Y. C.: 2022. Recent Advances in the Simulated Aging of Microplastics and Its Impact on Pollutant Adsorption Behavior. *Journal of Ecological and Environmenta*l *Sciences*, *31*(11): 2263. https://doi.org/.10.16258/j.cnki.1674-5906.2022.11.018

Keiluweit, M., Nico, P. S., Johnson, M. G. & Kleber, M.: 2010, Dynamic Molecular Structure of Plant Biomass-Derived Black Carbon (Biochar). *Environmental Science & Technology*, *44*, 1247-1253. https://doi.org/.10.1021/es9031419

Kleemann, N., Igansi, A., Silveira Jr, N., Pinto, L., Cadaval Jr, T., Arias, J., Barbosa, S., Primel, E. & Bamberg, A.: 2025, Simultaneous adsorption of polycyclic aromatic hydrocarbons (PAHs) on biochar from sewage sludge. *Environmental Science and Pollution Research International*, *32*, 8518-8528. https://doi.org/.10.1007/s11356-025-36255-

Kronberg, B.: 2016, The hydrophobic effect. *Current Opinion in Colloid & Interface Science*, *22*, 14-22. https://doi.org/.10.1016/j.cocis.2016.02.00

Li, C. Q., Ning, X. T., Yang, S. S., Shang, H.L., Yuan, F. & Sun, Z.M. 2024, Performance of FeS2/Kaolinite Composite Materials in the Degradation of Benzo[a]pyrene via Persulfate Activation. *Journal of Silicate Research*, *52*(10): 3093 - 3105. https://doi.org/.10.14062/j.issn.0454-5648.20240237

Li, D., Zhou, Y. a., Ding, H., Chang, L., Fu, N., Wang, X. & Tao, X.: 2022, Removing BaP from soil by biochar prepared with medicago and corn straw using batch and solid-phase extraction method. *Analytical Methods*, *14*, 4209-4218. https://doi.org/.10.1039/d2ay00823h

Lin, W., Fan, F. Q., Xu, G. M., Gong, K. Y., Cheng, X., Yuan, X. Y., Zhang, C., Gao, Y., Wang, S. R., Ng, H. Y. & Dong, Y.: 2023, Microbial community assembly responses to polycyclic aromatic hydrocarbon contamination across water and sediment habitats in the Pearl River Estuary. *Journal of Hazardous Materials*, *457*. https://doi.org/.10.1016/j.jhazmat.2023.131762

Liu, A., Feng, L.-J., Ou, Y., Zhang, X., Zhang, J. & Chen, H.: 2024, Competitive adsorption of polycyclic aromatic hydrocarbons on phosphorus tailing-modified sludge biochar provides mechanistic insights. *Environmental Geochemistry and Health*, *46*. https://doi.org/.10.1007/s10653-024-02283-x

Lu, Z., Chen, Z., Tian, W., Li, C., Zou, M., Zhang, R., Yang, K. & Bao, M.: 2025, Turn waste to wealth: Modification of coconut shells and waste diatomite from brewery for efficient adsorption of polycyclic aromatic hydrocarbons (PAHs) in seawater. *Separation and Purification Technology*, *362*. https://doi.org/.10.1016/j.seppur.2025.13181

Minkina, T., Vasilyeva, G., Popileshko, Y., Bauer, T., Sushkova, S., Fedorenko, A., Antonenko, E., Pinskii, D., Mazarji, M. & Ferreira, C. S. S.: 2022, Sorption of benzo a pyrene by Chernozem and carbonaceous sorbents: comparison of kinetics and interaction mechanisms. *Environmental Geochemistry and Health*, *44*, 133-148. https://doi.org/.10.1007/s10653-021-00945-

Obanla, O. R., Hestekin, J. A., Ojewumi, M. E., Bousrih, I. & Fawole, M. C.: 2023, Enhancing rubber (Hevea brasiliensis) seed shell biochar through acid-base modification for effective phenol removal from aqueous environments. *Results Eng*, *20*. https://doi.org/.10.1016/j.rineng.2023.10158

Premnath, N., Mohanrasu, K., Rao, R. G. R., Dinesh, G. H., Prakash, G. S., Ananthi, Ponnuchamy, K., Muthusamy, G. & Arun, A.: 2021, A crucial review on polycyclic aromatic Hydrocarbons - Environmental occurrence and strategies for microbial degradation. *Chemosphere*, *280*. https://doi.org/.10.1016/j.chemosphere.2021.130608

Puri, S., Thakur, I., Verma, A. & Barman, S.: 2021, Degradation of pharmaceutical drug paracetamol via UV irradiation using Fe-TiO2 composite photocatalyst: statistical analysis and parametric optimization. *Environmental Science and Pollution Research*, *28*, 47327-47341. https://doi.org/.10.1007/s11356-021-13895-

Qiu, H., Lv, L., Pan, B.-c., Zhang, Q.-j., Zhang, W.-m. & Zhang, Q.-x.: 2009, Critical review in adsorption kinetic models. *Journal of Zhejiang University-Science A*, *10*, 716-724. https://doi.org/.10.1631/jzus.A082052

Qiu, J. J., Hou, H. J., Liang, S., Yang, L., Gan, Q., Tao, S. Y., Yu, W. B., Lv, R. B., Ding, L., Xiao, K. K., Hu, J. P., Liu, B. C. & Yang, J. K.: 2022, Hierarchically porous biochar preparation and simultaneous nutrient recovery from sewage sludge via three steps of alkali-activated pyrolysis, water leaching and acid leaching. *Resources Conservation and Recycling*, *176*. https://doi.org/.10.1016/j.resconrec.2021.105953

Quach An, B. & Kajitvichyanukul, P.: 2019, Adsorption mechanism of dichlorvos onto coconut fibre biochar: the significant dependence of H-bonding and the pore-filling mechanism. *Water Science and Technology*, *79*, 866-876. https://doi.org/.10.2166/wst.2018.52

Revitt, D. M., Balogh, T. & Jones, H.: 2014, Soil mobility of surface applied polyaromatic hydrocarbons in response to simulated rainfall. *Environmental Science and Pollution Research*, *21*, 4209-4219. https://doi.org/.10.1007/s11356-013-2231-7

Simsek, S., Kaya, S., Katin, K. P., Ozer, A., Altunay, N., Brahmia, A., Senol, Z. M. & Ulusoy, H. I.: 2022, Theoretical and experimental insights about the adsorption of uranyl ion on a new designed Vermiculite-Polymer composite. *Journal of Molecular Liquids*, *352*. https://doi.org/.10.1016/j.molliq.2022.11872

Sun, T. T., Li, W. X. & Yin, K.: 2021, Estimation of total flux of polycyclic aromatic hydrocarbons facilitated by methane ebullition into water column from global lake sediments. *Water Research*, *204*. https://doi.org/.10.1016/j.watres.2021.117611

Tangsiri, R. & Nezamzadeh-Ejhieh, A.: 2020, Cadmium sulfide nanoparticles: Synthesis, brief characterization and experimental design by response surface methodology (RSM) in the photodegradation of ranitidine hydrochloride. *Chemical Physics Letters*, *758*. https://doi.org/.10.1016/j.cplett.2020.137919

Tian, R., Dong, H. R., Chen, J., Li, R. & Xie, Q. Q.: 2020, Amorphous Co3O4 nanoparticles-decorated biochar as an efficient activator of peroxymonosulfate for the removal of sulfamethazine in aqueous solution. *Separation and Purification Technology*, *250*. https://doi.org/.10.1016/j.seppur.2020.117246

Van Metre, P. C. & Mahler, B. J.: 2005, Trends in hydrophobic organic contaminants in urban and reference lake sediments across the United States, 1970-2001. *Environmental Science & Technology*, *39*, 5567-5574. https://doi.org/.10.1021/es0503175

Wang, K., Wang, Y., Zhang, S. Y., Chen, Y. D., Wang, R. P. & Ho, S. H.: 2022, Tailoring a novel hierarchical cheese-like porous biochar from algae residue to boost sulfathiazole removal. *Environmental Science and Ecotechnology*, *10*. https://doi.org/.10.1016/j.ese.2022.10016

Wang, W. J., Lin, J. X., Shao, S. B., Chen, H. J., Dai, J. W. & Yang, Y.: 2023, Enhanced adsorption of benzo(a)pyrene in soil by porous biochar: Adsorption kinetics, thermodynamics, and mechanisms. *Journal of Environmental Chemical Engineering*, *11*. https://doi.org/.10.1016/j.jece.2022.109002

Wang, X. Q., Wang, Y., Wang, W. & Li, Y. I.: 2025, Recent Advances in the Preparation, Modification, and Applications of Biochar. *Agricultural Engineering*, *15*(8): 58–67. https://doi.org/.10.19998/j.cnki.2095-1795.202508311

Wei, Z. H., Hou, C., Gao, Z. S., Wang, L. L., Yang, C. S., Li, Y. D., Liu, K. & Sun, Y. B.: 2023, Preparation of Biochar with Developed Mesoporous Structure from Poplar Leaf Activated by $KHCO_3$ and Its Efficient Adsorption of Oxytetracycline Hydrochloride. *Molecules*, *28*. https://doi.org/.10.3390/molecules2807318

Wu, B., Zhang, Y., Zhang, X. X. & Cheng, S. P.: 2011, Health risk assessment of polycyclic aromatic hydrocarbons in the source water and drinking water of China: Quantitative analysis based on published monitoring data. *Science of the Total Environment*, *410*, 112-118. https://doi.org/.10.1016/j.scitotenv.2011.09.046

Wu, C. L., Liu, J., Wang, Y., Zhao, Y. Q., Li, G. Q., Zhang, Y. F. & Zhang, G. J.: 2024, A clean method for controlling

pore structure development in potassium activation systems to improve CO_2 adsorption properties of biochar. *Science of the Total Environment*, *954*. https://doi.org/.10.1016/j.scitotenv.2024.176429

Yang, Q., Wang, T., Wang, J. W., Sui, Z. F., Wang, L. Z., Zhang, Y. S. & Pan, W. P.: 2021, Combustion, emission and slagging characteristics for typical agricultural crop straw usage in heating plants. *Thermochimica Acta, 702*. https://doi.org/.10.1016/j.tca.2021.178979

Ying, Z. W., Chen, X. W., Li, H., Liu, X. Q., Zhang, C., Zhang, J. & Yi, G. F.: 2021, Efficient Adsorption of Methylene Blue by Porous Biochar Derived from Soybean Dreg Using a One-Pot Synthesis Method. Molecules, 26. https://doi.org/.10.3390/molecules26030661

Yu, Q., Zhang, R., Deng, S., Huang, J. & Yu, G.: 2009, Sorption of perfluorooctane sulfonate and perfluorooctanoate on activated carbons and resin: Kinetic and isotherm study. *Water Research*, *43*, 1150-1158. https://doi.org/.10.1016/j.watres.2008.12.001

Yuan, C., Croft, K., de Nicola, S., Davis, A. P. & Kjellerup, B. V.: 2025, Treatment of polycyclic aromatic hydrocarbons (PAHs) and polychlorinated biphenyls (PCBs) in stormwater using polishing columns with biochar and granular activated carbon. *Chemosphere*, *372*, 144107. https://doi.org/.10.1016/j.chemosphere.2025.144107

Zhang, H. Y., Peng, B., Liu, Q. Y., Wu, C. S. & Li, Z. W.: 2022, Preparation of porous biochar from heavy bio-oil for adsorption of methylene blue in wastewater. *Fuel Processing Technology*, *238*. https://doi.org/.10.1016/j.fuproc.2022.107485

Zhang, S. S., Feng, Y. L., Sun, X. A., Hou, M. Z., Sun, P., Gu, Z. C. & Zhang, L. K.: 2026, Ginkgo Biloba Leaves Biochar Doped with K/Mg Promotes Peroxymonosulfate Activation for Tetracycline Removal in Aqueous Media Via Singlet Oxygen Generation. Water Air and Soil Pollution, 237. https://doi.org/.10.1007/s11270-026-09802-9

Zhang, X., Zhang, Z. F., Zhang, X. M., Yang, P. F., Li, Y. F., Cai, M. H. & Kallenborn, R.: 2021, Dissolved polycyclic aromatic hydrocarbons from the Northwestern Pacific to the Southern Ocean: Surface seawater distribution, source apportionment, and air-seawater exchange. *Water Research*, *207*. https://doi.org/.10.1016/j.watres.2021.117780

Zhang, Z. P., Tang, C. H., Wang, H. B., Zhong, M., Ge, P. C., Xu, W. L. & Chen, Y. Y.: 2024, Synthesis and Characterization of Potassium Bicarbonate and Urea-Modified Biochar from Rape Straw: Application in the Removal of Tetracycline from Aqueous Solution. *Water*, *16*. https://doi.org/.10.3390/w16172522

Zhou, D. L., Zhang, D., Zhang, M., Lü, T., Huang, J. G., Zhao, H. T. & Lin, J.: 2023, Efficient Treatment of PAH-Contaminated Water Using Magnetic-Modified Myriophyllum aquaticum Waste Biomass. *Water Air and Soil Pollution*, *234*. https://doi.org/.10.1007/s11270-023-06496-1

Zhu, L., Zhao, N., Tong, L. & Lv, Y.: 2018, Structural and adsorption characteristics of potassium carbonate activated biochar. Rsc Advances, 8, 21012-21019. https://doi.org/.10.1039/c8ra03335h

Supplementary Files

This is a list of supplementary files associated with this preprint. Click to download.

- Supplementarymaterial.docx